

Numerical Simulations of Solar Wind Disturbances by Coupled Models

D. Odstrcil, V. J. Pizzo

University of Colorado, LASP, 1234 Innovation Dr., Boulder, CO 80303, U.S.A.

C. N. Arge

AFRL, Kirtland AFB, NM, USA

M. M. Bissi, P. P. Hick, B. V. Jackson

UC San Diego, La Jolla, CA, USA

S. A. Ledvina, J. G. Luhmann

UC Berkeley, Berkeley, CA, USA

J. A. Linker, Z. Mikic, P. Riley

SAIC, San Diego, CA, USA

Abstract. Numerical modeling plays a critical role in efforts to understand the connection between solar eruptive phenomena and their impacts in the near-Earth space environment and in interplanetary space. Coupling the heliospheric model with empirical, observational, and numerical coronal models is described. Results show background solar wind, evolution of interplanetary transients, connectivity of magnetic field lines, and interplanetary shocks approaching geospace.

1. Introduction

Space weather is a coupled system of various phenomena with various spatial and temporal scales. Specialized physically based numerical models have been developed to address particular aspects of the entire problem. Currently, there is no single end-to-end numerical model connecting solar activity and Earth's magnetosphere. An integrated modeling approach is necessary to provide a complete picture suitable for interpretation of various remote and in-situ observations, and for development of forecasting capabilities. Coupling of existing codes promises to meet the above challenges.

2. Heliospheric model

The ENLIL (Sumerian god of wind) code is a numerical model for simulations of background solar wind (SW) and transient disturbances in the inner- and mid-heliosphere. The model is based on ideal magnetohydrodynamic (MHD)

description and the ratio of specific heats, γ , is usually chosen to be 1.5. Two additional continuity equations are used for tracing the injected material and the interplanetary magnetic field polarity, see (Odstrcil & Pizzo 1999a,b) for details. The explicit finite-difference, modified high-resolution, Total Variation Diminishing Lax–Friedrich (TVDLF) scheme (Toth 1996) is used on a fixed, uniform or non-uniform numerical grid. This scheme has no explicit artificial diffusion and produces second-order accuracy away from shocks and discontinuities, while simultaneously providing the stability that ensures non-oscillatory solutions. The field-interpolated central-difference approach for solving the magnetic field (Toth 2000) is used to satisfy $\nabla \cdot B = 0$ to round-off errors.

Large variations in plasma parameters between the Sun and Earth leads to regions with different processes and phenomena. We distinguish between the coronal and heliospheric regions with an interface located in the super-critical flow region (usually 18-35 solar radii, R_s). Construction of boundary conditions necessary to drive heliospheric computations is separated from ENLIL. Thus coupling with various analytic, empirical, and numerical models can be easily incorporated. ENLIL can provide outputs to magnetospheric and solar-energetic-particles (SEP) models (Luhmann et al. 2004).

3. Coupling with empirical coronal models

Accurate computation of the background SW parameters is crucial for predicting co-rotating structures and for transient disturbances that propagate and interact with those background structures. The Wang–Sheeley–Arge (WSA) model uses photospheric magnetic field data from the Mount Wilson Solar Observatory, Kitt Peak National Observatory, or Wilcox Solar Observatory, to calculate the radial magnetic field and flow velocity synoptic maps. The WSA model uses the potential field source surface model up to 2.5 R_s , Schatten Current Sheet model beyond 2.5 R_s , and an empirical relationship relating coronal parameters to SW speed, see Arge & Pizzo (2000) and Arge et al. (2004) for details. We derive the density and temperature values from the momentum flux and pressure balance across the inner boundary at 21.5 R_s . Background SW parameters are then computed by ENLIL (Fig. 1, left).

Coronal mass ejections (CMEs) observed by coronagraphs can be fitted by the so-called cone models (Zhao et al. 2002; Michalek et al. 2003; Xie et al. 2004). The fitted parameters (location, diameter, speed) together with the free parameters (maximum values and spatial profiles of the plasma density and temperature) enable simple specification of disturbances launched into the heliosphere. This approach facilitates direct control of impacts, and it is numerically robust and more accurate than empirical time-of-arrival formulae (e.g., Gopalswamy et al. 2001) due to realistic background SW and dynamic effects. We usually assume a spherical, homogeneous, over-pressured plasma cloud to construct time-dependent values at the inner boundary. The plasma cloud is launched along the IMF lines and it becomes significantly distorted by interaction with the background SW (see Fig. 1, right). Although this approach offers no information about the important internal magnetic structure of a CME, it provides easy, observationally-based model input. Heliospheric simulations then may provide the global context of transient disturbances within a co-rotating

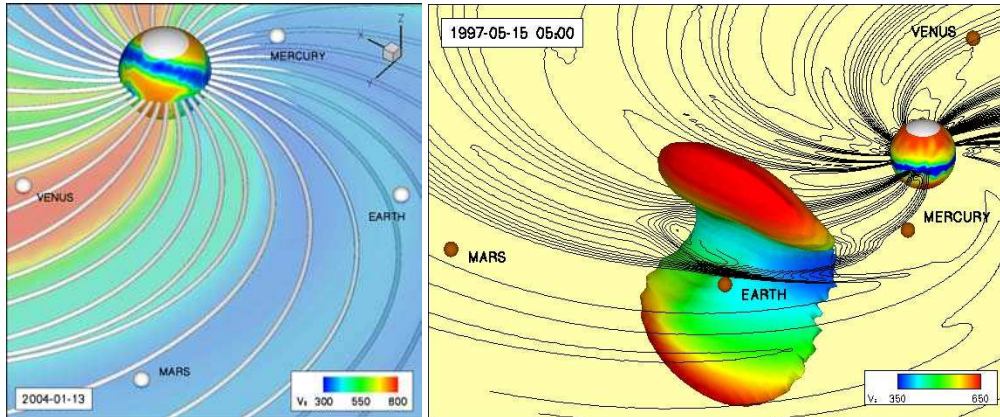


Figure 1. Background SW (left panel) visualized by flow velocity (color scale) in the equatorial plane and at the inner boundary, and by interplanetary magnetic field (IMF) lines (shaded white tubes). A nearly equatorial, heliospheric streamer belt is seen. Disturbed SW (right panel) visualized by ejecta (iso-surface at 25% of its maximum density) and flow velocity (contours in the equatorial plane and color scale at the inner boundary and on the ejecta boundary). A large distortion of the ejecta is caused by its interaction with the heliospheric streamer belt.

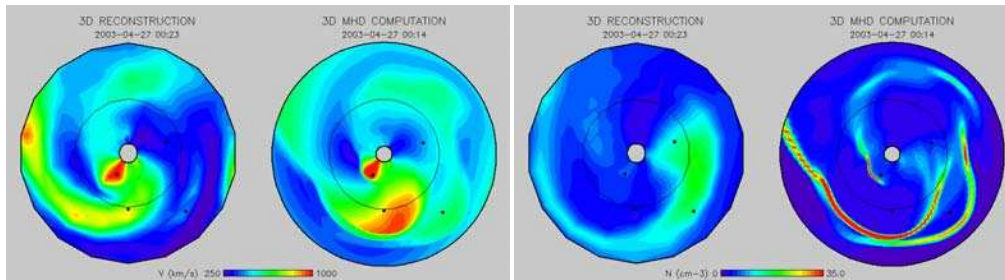


Figure 2. Comparison of SW flow velocity (left panel) and density (right panel) at the equatorial plane computed by tomographic reconstructions of IPS observations (left images) and by 3D MHD model (right images).

SW, positions of interplanetary shocks, and connectivity of the IMF line from geospace.

4. Coupling with observational heliospheric models

The heliospheric time-dependent tomographic model (Jackson & Hick 2002) developed at University of California at San Diego (UCSD) provides the SW density and velocity values up to 3 AU, as reconstructed from SMEI spacecraft and/or ground-based interplanetary scintillation (IPS) observations (provided by STELab at Nagoya University, Japan) using a kinematic SW model (Jackson & Hick 2002). We use these values at 35 Rs to construct time-dependent values at the inner boundary. Temperature is dynamically a minor factor in the helio-

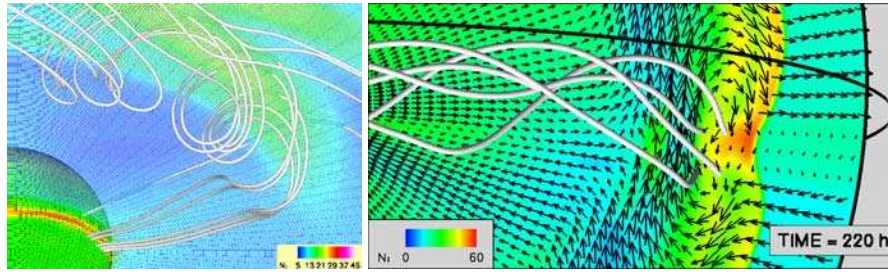


Figure 3. Selected IMF lines show an interplanetary magnetic flux rope which was generated by a hypothetical coronal magnetic eruption (MAS model) and launched into the heliosphere within the slower and denser, nearly equatorial, heliospheric streamer belt.

sphere and it is derived from balancing the total pressure. The magnetic field is taken from other coronal models. A challenging task is to reconstruct values of the density and velocity across the whole heliospheric inner boundary due to the many missing or out-of-range values.

Figure 2 shows simulation results of interplanetary events in April 2003. Global flow structures are similar to those provided by the UCSD reconstruction code; however, the 3-D MHD code simulates the dynamic interaction of co-rotating streams and formation of interplanetary shocks. Thus large velocity differences cause large dynamic compressions which lead to narrow density structures with large peaks. In the future, we might improve the tomographic reconstruction technique by replacing the kinematic SW model by the MHD model.

5. Coupling with numerical coronal models

The MAS (Magnetohydrodynamics Around Sphere) code is the 3-D MHD coronal model (Mikic & Linker 1994) which uses synoptic maps of the photospheric magnetic field provided by the Kitt Peak National Observatory. This code can also use empirical formulae for obtaining larger contrast between fast and slow SW streams (Riley et al. 2001). Recently, an improved description of the energy transport was incorporated to achieve more realistic coronal parameters emissions Mikic et al. (2007).

We construct time-dependent boundary values at the ENLIL inner boundary by extracting MAS data from a spherical shell at 30 Rs, the MAS outer boundary, interpolating between the MAS and ENLIL grids, and converting units. Since MAS generally neglects solar rotation, we have to synthesize the azimuthal magnetic field component in our inertial coordinate system. Numerical coupling (Odstrcil et al. 2004) worked well for the simulation of hypothetical transients (Fig. 3) as well as background SW with or without plasma clouds. In the first case, we have a large-scale magnetic structure launched into homogeneous SW, and in the second case, we have structured SW but without injected magnetic structures. We have encountered numerical difficulties when simulating the 12 May 1997 event which involves small-scale magnetic structures launched into a non-homogeneous SW. Because MAS and ENLIL each use

differing numerical techniques and grids, numerical inaccuracies result from the extrapolation of MAS results to ENLIL. Divergence cleaning techniques that ensure $\nabla \cdot \mathbf{B} = 0$ to truncation error are known to work on uniform grids and when reconnection is not of critical importance. However, it would be safer to insure $\nabla \cdot \mathbf{B} = 0$ to round-off from the beginning using staggered grids (Balsara & Kim 2004). This approach should enable more reliable coupling of different grids.

6. Coupling with SEP models

The IMF lines connecting geospace and interplanetary shocks and/or solar active regions are important for propagation and energization of solar energetic particles (SEPs). Values of MHD parameters along such IMF lines together with shock parameters can be directly used by SEP models (Luhmann et al. 2007).

Figure 4 shows that the geospace can be magnetically connected to a weak or a strong shock front (see color enhancement just beyond the shock) depending upon the rarefaction which stretches the IMF line towards the stronger shock region. The spiraling IMF line may lie at very large inclination angles to the bow-shaped shock front. Thus determination of shock parameters from MHD values stored along the IMF line is very difficult because many numerical grid points are needed to span across the shock structure, and pre- and post-shock values are at different parts of the SW stream. Accurate modeling of the topological connection of magnetic fields from the surface of the Sun to Earth and determination of shock parameters even at their weak flanks is needed.

7. Coupling with geospace models

Interplanetary shocks are thin structures which propagate through a huge spatial domain before hitting geospace. While shock arrival times can be predicted using a single numerical grid on available computer systems, a more sophisticated approach should be used for simulations in which shock thickness plays a role. Examples include calculations of local shock conditions required for calculations involving energetic particle energization or predicting the magnetospheric response.

A nested grid approach provides a practical solution when high resolution is required for features difficult to identify for automatic refinement. Figure 5 shows a system of nested grids with progressively finer resolution centered on geospace which is used to achieve a high resolution of interplanetary shocks hitting the magnetosphere. This is possible due to the self-steepening of shocks in each finer grid containing sufficient computational cells. The shock properties depend on local conditions and the driver, which is usually a very large structure. Thus, the shock structure and orientation can be computed with higher accuracy. Figure 5 shows a double-Mach stem formed in high resolution computations when the shock is distorted by the streamer belt and the shock front converges toward its axis. When contact discontinuities are important, the adaptive mesh refinement approach can be used with sophisticated refinement/de-refinement procedures.

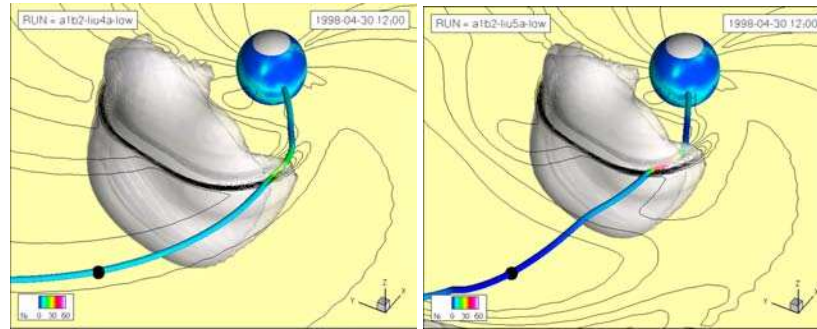


Figure 4. IMF connectivity between geospace and interplanetary shocks for two different scenarios; an ICME (white shaded structure) was launched into ambient co-rotating SW (left panel) and into SW disturbed by a preceding ICME (right panel). Normalized density is shown on the equatorial plane (black contours), at the inner boundary (colored), and an IMF line (colored) passing through Earth (small black sphere).

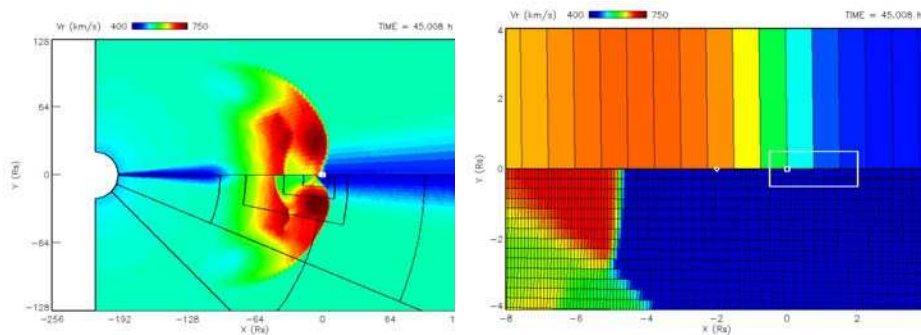


Figure 5. A hypothetical ICME propagating through a moderate streamer. Flow velocity (color scale) is shown in a global view (left) and in a detail view (right). Upper and lower half of each panel shows solution on a single and nested grids, respectively. Global (detail) view shows boundaries of the computational grids (individual numerical cells) as solid black lines. The L1-point, Earth position, and typical magnetospheric computational domain is marked by a white diamond, white square, and white box, respectively.

8. Conclusions

We have merged the ENLIL heliospheric model with the MAS, WSA, and UCSD coronal models of background state and transient disturbances. The ambient flow is supercritical at the models' interface, which facilitates coupling the simulations. These codes use different mathematical models, numerical methods, and computational grids, and the merging was demonstrated on various problems of practical interest. We did encounter some difficulties when coupling models with different grids in some computations. This points to limitations of the magnetic-field reconstruction technique used to maintain $\nabla \cdot \mathbf{B} = 0$ and to inaccuracies of the interpolation procedure at grid interfaces. We will revise

our numerical approach to ensure accurate simulation of the IMF connectivity through various computational domains and small-scale magnetic structures.

Although the coupling approach represents a revolutionary concept which has only recently permitted the simulation of selected space-weather events, it is not clear whether some physics might be distorted or filtered-out during coupling between different physical models and different numerical grids. There is a need for coupled coronal and heliospheric phenomena to be simulated by a single model without coupling different physical models and numerical grids. This would provide benchmarking and verification scenarios for coupled codes and their frameworks.

Acknowledgments. This work has been supported by AFOSR/MURI, NASA/LWS, and NSF/CISM projects. We acknowledge data from Mount Wilson and Kitt Peak Solar observatories, ESA-NASA SOHO/LASCO and USAF Coriolis/SMEI spacecraft instruments, Nagoya University STELab/IPS radio antennas, and NASA National Space Science Data Center.

References

- Arge, C. N., & Pizzo, V. J. 2000, *J. Geophys. Res.*, 105, 10465
- Arge, C. N., Luhmann, J. G., Odstrcil, D., Schrijver, C. J., & Li, Y. 2004, *J. Atmos. Terr. Phys.*, 66, 1295
- Balsara, D. S., & Kim, J. 2004, *ApJ*, 602, 1079
- Gopalswamy, N., Lara, A., Yashiro, S., Kaiser, M. L., & Howard, R. A. 2001, *J. Geophys. Res.*, 106, 29207
- Jackson, B. V., & Hick, P. P. 2002, *Solar Phys.*, 211, 345
- Luhmann, J. G., Solomon, S. C., Linker, J. A., Lyon, J. G., Mikic, Z., Odstrcil, D., Wang, W., & Wiltberger, M. 2004, *J. Atmos. Terr. Phys.*, 66, 1243
- Luhmann, J. G., Ledvina, S. A., Krauss-Varban, D., Odstrcil, D., & Riley, P. 2007, *Adv. Space Res.*, 40(3), 295
- Michalek, G., Gopalswamy, N., & Yashiro, S. 2003, *ApJ*, 584, 472
- Mikic, Z., & Linker, J. A. 1994, *ApJ*, 430, 898
- Mikic, Z., Linker, J. A., Lionello, R., Riley, P., & Titov, V. 2007, in *Astronomical Society of the Pacific Conf. Ser.* 370, *Solar and Stellar Physics Through Eclipses*, ed. O. Demircan, S. O. Selam & B. Albayrak (San Francisco: ASP), 299
- Odstrcil, D., & Pizzo, V. J. 1999a, *J. Geophys. Res.*, 104, 483
- Odstrcil, D., & Pizzo, V. J. 1999b, *J. Geophys. Res.*, 104, 28225
- Odstrcil, D., Pizzo, V. J., Linker, J. A., Riley, P., Lionello, R., & Mikic Z. 2004, *J. Atmos. Terr. Phys.*, 66, 1311
- Riley, P., Linker, J. A., & Mikic, Z. 2001, *J. Geophys. Res.*, 106, 15889
- Toth, G., & Odstrcil, D. 1996, *J. Comput. Phys.*, 128, 82
- Toth, G. 2000, *J. Comput. Phys.*, 161, 605
- Xie, H., Ofman, L., & Lawrence, G. 2004, *J. Geophys. Res.*, 109, doi:10.1029/2003JA010226
- Zhao, X. P., Plunkett, S. P., & Liu, W. 2002, *J. Geophys. Res.*, 107, doi:10.1029/2001JA009143